Yrast states of the proton drip line nucleus ^{106}Sb

D. Sohler,[1] J. Cederkäll,[2] M. Lipoglavšek,[3,4] Zs. Dombrádi,[1] M. Górska,[5,6] J. Persson,[7] D. Seweryniak,[8] I. Ahmad,[8] A. Atac,[7] R. A. Bark,[9] J. Blomqvist,[2] M. P. Carpenter,[8] B. Cederwall,[2] C. N. Davids,[8] C. Fahlander,[3] S. M. Fischer,[8] H. Grawe,[5] G. Hackman,[8] R. V. F. Janssens,[8] A. Johnson,[2] A. Kerek,[2] W. Klamra,[2] J. Kownacki,[10] C. J. Lister,[8] S. Mitarai,[11] D. Nisius,[8] L.-O. Norlin,[2] J. Nyberg,[12] G. Poli,[13] P. Reiter,[8] J. J. Ressler,[14] H. A. Roth,[15,16] J. Schwartz,[8] G. Sletten,[9] J. Uusitalo,[8] W. B. Walters,[14] and M. Weiszflog[12]

[1]*Institute of Nuclear Research, 4001 Debrecen, P.O. Box 51, Hungary*
[2]*Physics Department, Royal Institute of Technology, Stockholm, Sweden*
[3]*Department of Cosmic and Subatomic Physics, Lund University, Lund, Sweden*
[4]*J. Stefan Institute, Ljubjana, Slovenia*
[5]*Gesellschaft für Schwerionenforschung, Darmstadt, Germany*
[6]*Institute of Experimental Physics, University of Warsaw, Warsaw, Poland*
[7]*Department of Radiation Science, Uppsala University, Uppsala, Sweden*
[8]*Argonne National Laboratory, Argonne, Illinois 60439*
[9]*Niels Bohr Institute, University of Copenhagen, Copenhagen, Denmark*
[10]*Heavy Ion Laboratory, University of Warsaw, Warsaw, Poland*
[11]*Department of Physics, Kyushu University, Fukuoka, Japan*
[12]*The Svedberg Laboratory, Uppsala University, Uppsala, Sweden*
[13]*Istituto Fisica Generale Applicata, University Milano, Italy*
[14]*University of Maryland, College Park, Maryland 20742*
[15]*Department of Physics, Chalmers University of Technology, Gothenburg, Sweden*
[16]*Gothenburg University, Gothenburg, Sweden*

(Received 28 August 1998)

Yrast states of ^{106}Sb have been investigated in the ^{54}Fe(^{58}Ni,αpn) reaction using in-beam γ-spectroscopic methods and in the ^{50}Cr(^{58}Ni,pn) reaction performing delayed γ and conversion electron studies. A new isomeric state was found at 103 keV with $t_{1/2}=232(21)$ ns. The number of states and transitions in the proposed level scheme have been doubled. The experimental results are discussed within the framework of the shell model. [S0556-2813(99)08502-7]

PACS number(s): 21.10.Hw, 23.20.Lv, 27.60.+j, 21.60.Cs

I. INTRODUCTION

A theoretically and experimentally equally challenging direction in nuclear spectroscopy is the study of nuclei close to the limits of stability. In heavy nuclei the location of the proton drip line has been established in the $A=100$ and 150 [1] regions. The nuclei ^{105}Sb and ^{109}I are ground-state proton emitters [2,3]. In the present work the structure of the next to drip line nucleus ^{106}Sb has been investigated by γ-spectroscopic methods. Prior to this study the only information on this nucleus was a cascade of four γ-rays, observed in a previous NORDBALL experiment [4].

II. EXPERIMENTAL METHODS AND RESULTS

Two experiments were performed to investigate the structure of nuclei close to the $N=Z=50$ shell closure. The first one was an in-beam measurement performed at the Tandem Accelerator Laboratory of the Niels Bohr Institute using EUROBALL cluster detectors. Its aim was to obtain more information on the structure of nuclei near ^{100}Sn by analyzing $\gamma\gamma$-coincidence relations and angular distributions of γ rays. The application of a rather wide time window of 474 ns made possible to search for medium-long isomeric states as well. The second experiment, performed at the Argonne National Laboratory, was focused on a study of long-lived isomeric states in the neighborhood of ^{100}Sn by detection of γ rays and conversion electrons from mass-analyzed recoils.

A. In-beam experiment

In the in-beam experiment neutron deficient nuclei were produced by bombarding a ^{54}Fe target with a ^{58}Ni beam at 261 MeV. A 3.0-mg/cm^2-thick target was isotopically enriched to 99.9% and placed on a 21.8-mg/cm^2 Au backing. The target was surrounded by three detector systems. The evaporated charged particles were detected in 31 thin Si detectors almost completely surrounding the target. Neutrons emitted from the compound nuclei were detected in a neutron multiplicity filter consisting of 16 neutron detectors covering a solid angle of 1.4π downstream of the target position. The Si-detector system, as well as the neutron multiplicity filter, were described in Refs. [5–8]. The four Ge cluster detectors [9] were mounted upstream of the target position in a closely packed geometry with a common focus of the central capsules at 21 cm from the center of each cluster. To optimize the γ-ray detection efficiency, the target position was moved 10 cm toward the Ge detectors along the beam line. Each cluster contains seven Ge crystals. Totally 25 of the 28 available crystals worked during the experiment. The setup had a photopeak efficiency of 7.9(3)% at 1.3 MeV, according to a simulation performed with the GEANT code [10].

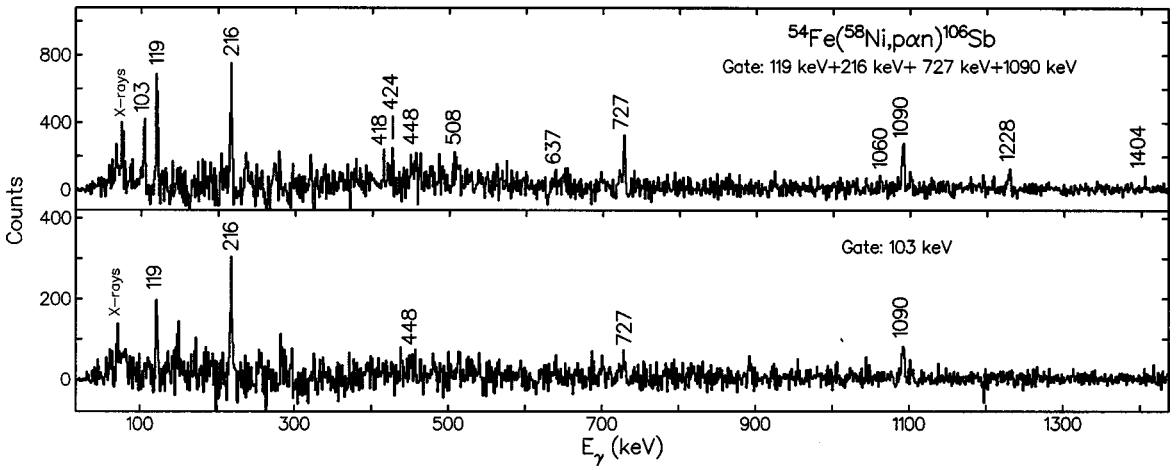

FIG. 1. Sum of the gates set on the 119-, 216-, 727-, and 1090-keV transitions (a), and the spectrum gated with the 103-keV γ ray assigned to ^{106}Sb (b).

The time reference signal was given either by a γ ray hitting the neutron multiplicity filter or by a charged particle hitting one of the Si detectors. The trigger condition demanded that at least one γ ray was detected in the Ge crystals at the same time as at least one neutron was identified on line by the neutron multiplicity filter. Totally, 2.5×10^9 events were collected at a rate of 7.5×10^3 events/s with an average γ-ray fold of 2.5.

The coincidence events were sorted into a set of E_γ-E_γ matrices, requiring different conditions on the number of detected charged particles and neutrons. In the data analysis the sum of the $1\alpha1n$- and $1\alpha1p1n$-gated matrices were used. γ-rays were assigned to the ^{106}Sb nucleus if they were in coincidence with the previously known transitions [4]. All γ rays assigned to ^{106}Sb are shown in Fig. 1(a). The spectrum was obtained by summing gates set on the 119-, 216-, 727-, and 1090-keV transitions. In Fig. 1(b) the spectrum obtained by putting the gate on the new 103-keV transition can be seen.

The level scheme of ^{106}Sb shown in Fig. 2 was constructed mainly on the basis of the $\gamma\gamma$-coincidence relations. The 103-keV transition, being in coincidence with the strongest transitions in ^{106}Sb, was proven to be delayed with a half-life of 232 ns (see Sec. II B), while the other transitions were prompt. Therefore, the 103-keV γ ray was assigned to the decay of the first excited state of ^{106}Sb. The cascade of the four strongest transitions observed previously [4] is placed on the top of the isomeric state. The yrast cascade is continued by two additional γ rays up to an excitation energy of about 4 MeV. The new transitions are put in order of decreasing intensity. In addition to the yrast cascade, a side branch connected to the levels at 438 and 1528 keV was observed. Besides the transitions placed in the level scheme, γ rays with energies of 424, 637, and 1404 keV were also assigned to ^{106}Sb on the basis of the $\gamma\gamma$-coincidence relations. However, due to the low statistics their positions in the level scheme are uncertain.

The multipolarities of the observed transitions were determined by means of angular distribution ratios. The detector elements of the clusters created three rings at $\sim135^o$, $\sim120^o$, and $\sim100^o$ relative to the beam direction. γ-ray spectra, gated with different combinations of detected particles, were sorted for the three detector angles. The intensity ratios $R_1=I_\gamma(135^o)/I_\gamma(120^o)$ and $R_2=I_\gamma(135^o)/I_\gamma(100^o)$ were used to determine the angular momenta transferred by the γ rays. The ratios formed two groups with values $R_1\approx0.87$, $R_2\approx0.75$, and $R_1\approx1.03$, $R_2\approx1.15$, respectively, with relative errors of about 10% for the stronger transitions. The former group corresponds to stretched dipole and the latter to stretched quadrupole transitions for γ rays with known multipolarity in ^{107}Sn, ^{108}Sb, and ^{109}Te. The two-dimensional plot of the R_1 and R_2 ratios, shown in Fig. 3, made it possible also to draw definite conclusions in the case

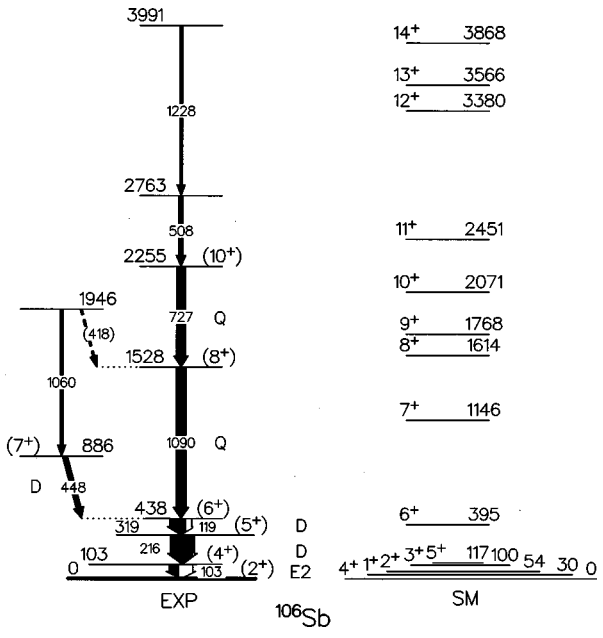

FIG. 2. Experimental and theoretical level schemes of ^{106}Sb. The widths of the arrows show the intensities obtained from the coincidence matrix. The unfilled part of the 103-keV arrow represents the intensity of the conversion electrons for pure $E2$ multipolarity. The multipolarities of the transitions are also given. D marks dipole transitions, and Q marks quadrupole transitions. All the spin values are tentative. They are given relative to the assumed ground state spin $I^\pi=2^+$. The theoretical level scheme is calculated in the framework of the shell model.

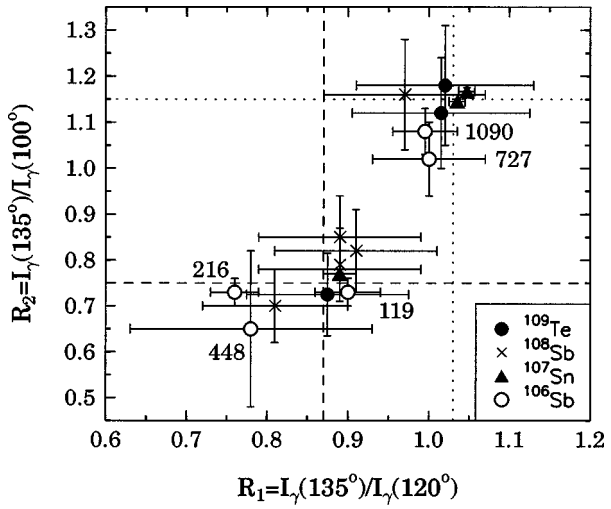

FIG. 3. Two-dimensional plot of the angular distribution ratios. The two kinds of dashed lines indicate the weighted average values for dipole and quadrupole transitions obtained from ratios of γ rays with known multipolarities. The ^{106}Sb transitions are labeled with their energies given in keV.

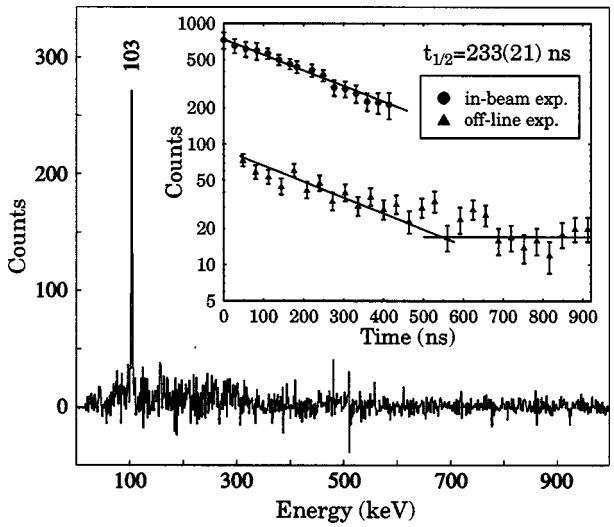

FIG. 4. Background subtracted γ-ray spectrum obtained in the off-line experiment. The time window was set from 0 to 500 ns after the recoiling nucleus hit the catcher foil. The time distribution of the intensity of the 103-keV γ ray obtained in the in-beam experiment (marked by circles), and the time spectrum of the same transition from the off-line experiment (marked by triangles), are shown as an inset.

of weak transitions. Dipole character was assigned to the 119-, 216-, and 448-keV transitions, while the angular distribution ratios for the 727- and 1090-keV γ rays suggest quadrupole nature. The spins of the states were assigned assuming that all observed transitions are stretched, and that the spins increase with increasing excitation energy.

B. A new isomeric state in ^{106}Sb

Isomeric states of residual nuclei produced in the ^{50}Cr $+^{58}$Ni reaction on a 0.56-mg/cm^2 thick target at beam energy of 220 MeV were studied after separation using the fragment mass analyzer (FMA) at the Argonne National Laboratory [11]. The FMA is set up so that every fourth mass overlaps in the focal plane. In the present case it was configured to allow nuclei with $A=94$, 98, 102, and 106 to pass through. The mass over charge ratio of the recoiled ions was obtained from their positions in front of the focal plane as measured by a position-sensitive detector. The recoiled nuclei were stopped in the focal plane by a 3.6-mg/cm^2-thick Al foil. The typical flight time of a recoiling nucleus between the target and the catcher foil was about 640 ns. Conversion electrons from the decay of isomeric states were measured by five silicon *p-i-n* diodes forming five sides of a cube with a size of 2.5 cm behind the catcher foil. The electron detection efficiency was about 15% in the 80-160-keV energy range. Four Ge detectors at ~ 3 cm from the center of the catcher foil, having a total photo peak efficiency of about 5% at 1.3 MeV, detected the delayed γ rays. Events were stored on tape if at least one electron or one γ-ray detector fired within 2 μs after a heavy ion had passed through the multiwire proportional counter detector [12] placed between the slits and the focal plane.

The background subtracted γ-ray spectrum is shown in Fig. 4. In the corresponding electron spectrum two lines were observed, the K and L conversion electron lines of the 103 keV transition. The total conversion coefficient obtained from the ratio of the electron intensity over γ-ray intensity was 1.8(2). The theoretical values for $E1$, $M1$, $E2$, and $M2$ multipolarities are 0.18, 0.58, 1.51, and 5.81, respectively. Thus $E2$ multipolarity can be assigned to the 103-keV transition. The half-life of the initial state of this transition was determined from the time spectrum of the Ge detectors, shown in the lower part of the inset in Fig. 4. The fit gives $t_{1/2}=230(30)$ ns for the half-life, in accordance with the result obtained from the time spectrum of the electron detectors. The time distribution of the intensity of the 103-keV γ ray obtained from the time spectrum of the Ge cluster detectors in the in-beam experiment can be seen in the upper part of the insert in Fig. 4. From these data the half-life of the isomeric state was measured to be $t_{1/2}=235(30)$ ns in agreement with the FMA data. Taking the weighted average of the measured values a half-life of $t_{1/2}=232(21)$ ns was assigned to the isomeric state at 103 keV. From the measured half life and the transition energy, an $E2$ transition strength of 2.8(3) W.u. can be deduced.

C. Discussion of the level scheme

The experimental results were compared to a shell model calculation performed with the Ritsschil package using the same matrix elements as in our previous calculations of Sb isotopes [4,13]. Especially for the interaction, modified surface delta interaction (MSDI) matrix elements were used with strength parameters $A_0=A_1=0.32$ MeV and monopole shifts $B_0=-3B$ and $B_1=B$ with $B=0.32$ MeV. The model space comprised the neutron $d_{5/2}$, $g_{7/2}$, $s_{1/2}$, and $d_{3/2}$ shells, while protons were allowed only in the $d_{5/2}$ and $g_{7/2}$ states. The calculated yrast states are shown in Fig. 2 together with the experimental data.

The ground state of ^{106}Sb is expected to arise from coupling the odd proton to the odd neutron situated in the $d_{5/2}$ state. In the shell model calculation the splitting of this multiplet is very compressed, all the $I^\pi=0^+-5^+$ members of the multiplet are below 310 keV, and their splitting can be approximated with an open up parabola characteristic for a

particle-hole multiplet. The energy splitting of the $\pi d_{5/2}\nu g_{7/2}$ multiplet is also fairly flat (spread over 290 keV), and has some staggering. The $\nu d_{5/2}$ and $g_{7/2}$ orbits are almost degenerate in ^{101}Sn, as extrapolated from a shell model analysis of the light Sn to Cd isotopes [13]. As these orbitals are filled simultaneously with increasing neutron number, the neutron quasiparticle states are mixtures of configurations with the odd neutron ($d_{5/2}$ or $g_{7/2}$) coupled to varying pairs of neutrons in the $d_{5/2}$ and $g_{7/2}$ orbits, respectively. Therefore, the members of the multiplets are not well separated, and the parabolic shape is not well developed. The energy difference of the respective states varies from 110 keV for $I^\pi=2^+$ to about 195 keV for $I^\pi=5^+$. The $\pi d_{5/2}\nu d_{5/2}$ configuration is favored for $I<5$. According to the shell model, the $\pi g_{7/2}\nu g_{7/2}$ multiplet can be approximated with an open down parabola, and its highest spin member is the yrast 7^+ state. The yrast 8^+,9^+, and 10^+ states are predicted to arise from broken neutron pair configurations.

In the experimental level scheme there is a set of states below 450 keV with a total spin difference of 4. In a previous prompt spectroscopy experiment [4] the 119–216-keV cascade, in analogy to a similarly tentative assignment in ^{108}Sb [14], was assigned to a (6^+)-(5^+)-(4^+) level sequence. For ^{108}Sb from β^+/EC decay data [15] it can be concluded that the ground state spin is $I\geqslant 4$. From the 0.6 ± 0.2 s lifetime of the ^{106}Sb ground state [16] $I\leqslant 2$ is expected for its spin. Although the shell model predicts 4^+ for the ground state, due to the flattening of the energy splitting and the asymmetry in the pn multiplets, favoring low-spin states energetically, going from ^{108}Sb to ^{106}Sb, the $I^\pi=2^+$ state can be expected to cross the $I^\pi=4^+$ level to become the ground state. Consequently, tentative spin-parity values $I^\pi=(4^+)$, (5^+), (6^+), (7^+), (8^+), and (10^+) can be assigned to the states at 103, 319, 438, 886, 1528, and 2255 keV, respectively. With these assignments the wave functions of the (2^+) ground state and the (4^+) state at 103 keV are dominated by the $\pi d_{5/2}\nu d_{5/2}$ configuration. The (5^+) and (6^+) levels at 319 and 438 keV, respectively, are interpreted as members of the $\pi d_{5/2}\nu g_{7/2}$ multiplet. The wave function of the above-mentioned shell model states contains these configurations with $>55\%$ weight. The (7^+) level at 886 keV corresponds to the yrast 7^+ shell model state, with the dominating ($>65\%$) $\pi g_{7/2}\nu g_{7/2}$ configuration calculated at ~ 1150 keV.

Using the effective proton and neutron $E2$ charges from previous work [13], $e_p=1.72e$ and $e_n=1.44e$, the $B(E2;4^+\rightarrow 2^+)$ is calculated as 3.6 W.u., in fair agreement with the experimental value 2.8(3) W.u. The $E2$ strength corroborates the configuration assignments of the (2^+) and (4^+) states to the same $\pi d_{5/2}\nu d_{5/2}$ configuration, as major admixtures of the $g_{7/2}$ orbital would imply $g_{7/2}\leftrightarrow d_{5/2}$ spin-flip $E2$ transitions, which are weak. A detailed inspection of the shell model result reveals a dominating neutron contribution to the reduced $E2$ matrix element, which is responsible for the enhanced $E2$, as observed earlier in the Sn isotopes [13].

In the shell model calculation both of the multiplets $\pi d_{5/2}\nu d_{5/2}$ and $\pi d_{5/2}\nu g_{7/2}$, respectively, exhibit a low-lying 1^+ state. The assignments adopted in Fig. 2, and discussed so far, explain why an excited $I^\pi=1^+$ is not populated in the yrast cascade from high-spin states. On the basis of the experimental data and in view of the uncertainties in the MSDI shell model approach, it cannot be excluded that the ground state is a 1^+ state, which would reduce the spins in Fig. 2 by 1. In this case, tentative spin-parity values $I^\pi=(3^+)$, (4^+), (5^+), (6^+), (7^+), and (9^+) can be assigned to the states at 103, 319, 438, 886, 1528 and 2255 keV, respectively. The (1^+) state would be assigned to the $\pi d_{5/2}\nu d_{5/2}$ configuration. The shell model description is somewhat worse than in the case with the assumption of a (2^+) ground state.

ACKNOWLEDGMENTS

This work was supported by the Swedish and Danish Natural Science Research Councils, the Hungarian Fund for Science Research (OTKA Contract No. 20655), and by the U.S. Department of Energy, Nuclear Physics Division (Contract Nos. W-31-109-ENG-38 and No. DE-FG02-94-ER49834).

[1] P. J. Woods and C. N. Davids, Annu. Rev. Nucl. Part. Sci. **47**, 541 (1997).
[2] R. J. Tighe, D. M. Moltz, J. C. Batchelder, T. J. Ognibene, M. W. Rowe, and J. Cerny, Phys. Rev. C **49**, R2871 (1994).
[3] A. Gillitzer, T. Faestermann, K. Hartel, P. Kienle, and E. Nolte, Z. Phys. A **326**, 107 (1987).
[4] D. Seweryniak *et al.*, Phys. Lett. B **321**, 323 (1994).
[5] G. Sletten, *Proceedings of the International Seminar on the Frontier of Nuclear Spectroscopy*, Kyoto, 1992 (World Scientific, Singapore, 1993).
[6] T. Kuroyanagi, S. Mitarai, S. Suematsu, B. J. Min, H. Tomura, J. Mukai, T. Maeda, and R. Nakatani, Nucl. Instrum. Methods Phys. Res. A **316**, 289 (1992).
[7] S. E. Arnell, H. A. Roth, and Ö. Skeppstedt, Nucl. Instrum. Methods Phys. Res. A **300**, 303 (1991).
[8] D. Wolski, M. Moszynski, T. Ludziejewski, A. Johnson, W. Klamra, and Ö. Skeppstedt, Nucl. Instrum. Methods Phys. Res. A **360**, 584 (1995).
[9] J. Eberth *et al.*, Prog. Part. Nucl. Phys. **38**, 29 (1997).
[10] R. Brun *et al.*, GEANT detector description and simulation tool, CERN Program Library, Long Writeup, W5013 (CERN, Geneva, 1996).
[11] C. N. Davids *et al.*, Nucl. Instrum. Methods Phys. Res. B **70**, 358 (1992).
[12] M. Lipoglavšek *et al.*, Phys. Lett. B **440**, 246 (1998).
[13] H. Grawe, R. Schubart, K. H. Maier, and D. Seweryniak, Phys. Scr. **T56**, 71 (1995).
[14] A. Johnson *et al.*, Nucl. Phys. **A557**, 401c (1993).
[15] M. Shibata *et al.*, Phys. Rev. C **55**, 1715 (1997).
[16] M. Lewitowicz, in *Proceedings of International Conference on Exotic Nuclei and Atomic Masses* (ENAM 95), edited by M. de Saint-Simon and O. Sorlin (Editions Frontières, Gif-sur-Yvette, 1995), p. 427.